

1 **Mapping Soil Erodibility over India**

2
3
4
5 Ravi Raj¹, Manabendra Saharia^{1,2} Sumedha Chakma¹

6
7
8 ¹Department of Civil Engineering, Indian Institute of Technology Delhi, Hauz Khas, New
9 Delhi 110016, India

10 ²Yardi School of Artificial Intelligence, Indian Institute of Technology Delhi, Hauz Khas,
11 New Delhi 110016, India

12
13
14
15
16
17
18 Submitted for publication in CATENA
19

20
21
22
23
24 **Corresponding Author:**

25 Dr. Manabendra Saharia

26 Indian Institute of Technology Delhi

27 Hauz Khas, New Delhi, India 110016

28 Email: msaharia@iitd.ac.in

29

30 Abstract:

31 Soil erosion is a major environmental problem worldwide, and almost half of India's total
32 geographical area is susceptible to it. The Revised Universal Soil Loss Equation (RUSLE) has
33 been widely used globally to estimate soil erosion, and Soil erodibility factor, denoted by K-
34 factor, is an essential component of RUSLE. Although previous studies have assessed soil
35 erodibility in India, they have been limited to small scales such as watersheds or districts. A
36 national scale assessment of soil erodibility doesn't exist and is critical to developing a
37 systematic understanding of soil erosion over India. In this study, we estimated soil erodibility
38 factors over India using RUSLE Nomograph and Environmental Policy Integrated Climate
39 (EPIC) model approaches at a high resolution of 250 m. Our results showed that the K-factor
40 estimated using the Nomograph approach was more accurate than the observed soil erodibility
41 factors. Additionally, we developed erodibility indices such as CR (Clay Ratio), MCR
42 (Modified Clay Ratio), and CLOM (Critical Level of Organic Matter) to assess their sensitivity
43 with respect to soil erodibility factors. Finally, we created a susceptibility to erosion map over
44 India using CLOM index classification. The national average soil erodibility factor for India is
45 estimated to be 0.028 t-ha-h/ha/MJ/mm. Histosols soil type is the least susceptible to erosion,
46 while Xerosols soil type is most susceptible among the prevalent soil classes in India. This is
47 the first national-scale mapping of soil erodibility over India, providing an essential asset for
48 soil conservation and erosion management planning by experts.

49 **Key words:** Soil erodibility factor,
50 Clay Ratio, Modified Clay Ratio, Critical Level of Organic Matter, India, Soil erosion

51

52 **Highlights:**

- 53 • First national-scale mapping of soil erodibility over India.
54 • K-factor estimated using the widely used Nomograph and EPIC models.

- 55 • The average soil erodibility factor for India was estimated to be 0.028 t-ha-
- 56 h/ha/MJ/mm.
- 57 • CLOM index highly correlated with soil erodibility in Indian condition.
- 58 • A susceptibility to soil erosion map was also created based on CLOM index over India.
- 59
- 60
- 61

62 **1. Introduction**

63 Soil erosion is a major trigger for land degradation and has been identified as one of the leading
64 environmental problems, the globe is facing (Borrelli et al., 2020; Choudhury et al., 2021;
65 Ghosh et al., 2012; Ma et al., 2003; Salesa and Cerdà, 2020; Smetanová et al., 2019). Soil
66 erosion contributes around 15-30 billion tons of sediment which is transported annually by the
67 major rivers of the world into oceans, accounting for approximately 46% of the total land
68 degradation (Kulimushi et al., 2021). In India, approximately 45% of the total geographical
69 area of the nation is susceptible to soil erosion (Bhattacharyya et al., 2015). Numerous physical
70 and empirical models have been developed and implemented worldwide to estimate soil
71 erosion coupled with remote sensing and geographic information system (GIS) systems
72 covering a wide range of spatio-temporal scales (Flanagan et al., 2012; Jiang et al., 2019;
73 Kazamias and Sapountzis, 2017; Kumar and Singh, 2021; Lobo and Bonilla, 2019; Nearing et
74 al., 1989; Saghafian et al., 2015). Climate and soil properties also influence the erosion induced
75 by water (Borrelli et al., 2020; Guo et al., 2019; Nearing et al., 2005; Senanayake and Pradhan,
76 2022). The Universal Soil Loss Equation (USLE) (Wischmeier and Smith, 1978) and Revised
77 Universal Soil Loss Equation (RUSLE) (Renard et al., 1991) empirical models are widely used
78 to estimate long-term annual soil loss. These two models (USLE and RUSLE) require less
79 input datasets, robust, and simple to use even at large scales (Balasubramani et al., 2015). Soil
80 erodibility (K-factor) is one of the important factors of the RUSLE model. A national scale
81 assessment of soil erodibility will be helpful in planning and implementing watershed
82 management activities to deal with soil erosion problem which is currently missing over India.
83 In this study, soil erodibility factor has been modelled over India using gridded datasets at 250
84 m spatial resolution. This study will complement the rainfall erosivity mapping by Raj et al.,
85 (2022) in developing a systematic and comprehensive understanding of soil erosion in India.

86 Soil erodibility is the response of the soil profile to the erosivity induced by rainstorms and
87 reflects the combined effect of rainfall, infiltration, and runoff on soil erosion (Bonilla and
88 Johnson, 2012). Soil erodibility is a composite property of soil, determined by a wide range of
89 associated parameters, but only some of these parameters are directly related to the soil types
90 (Veihe, 2002). Ideally, soil erodibility factors would be best calculated from direct field
91 measurements with the help of natural runoff diagrams but getting these types of records for
92 long-term studies are too expensive and time-consuming (Dangler and El-Swaify, 1976;
93 Efthimiou, 2020; Torri et al., 1997; Young and Mutchler, 1977). So, various attempts had been
94 made to correlate soil properties with the measured soil erodibility factors (Cohen et al., 2005;
95 Wang et al., 2022). The widely adopted relationship to estimate K-factor is the soil erodibility
96 nomograph approach (Wischmeier and Smith, 1978) which uses more easily obtainable
97 datasets such as soil texture, structure, permeability and SOM (soil organic matter) (Efthimiou,
98 2020). Soil erodibility factors were also estimated by Torri et al., (1997) using clay content of
99 the soil, soil organic matter (SOM), and the Napierian logarithm of the geometric mean particle
100 diameter. Romkens et al., (1986) developed a relation depending upon four regression
101 coefficients and particle size distribution to estimate soil erodibility factors. An equation was
102 also developed by Mulengera and Payton (1999) to calculate K-factor for tropical regions using
103 SOM, soil permeability and soil texture data. Although these models were estimating soil
104 erodibility values with various degrees of excellence, but could not provide the distribution of
105 soil erosion spatially due to the complex environment of the model, and hence not suitable for
106 modelling over larger areas (Lu et al., 2004).

107 Predicting soil erodibility factor spatially, and its geospatial upscaling is very sensitive to the
108 methods and models used in the study. The properties of soil which directly control K-factors
109 are shear strength, porosity, organic matter, permeability, bulk density, shape and size of
110 aggregates, particle size distribution, and chemical composition of soil (Chen and Zhou, 2013).

111 The performance of the models depends on the physical, biological, mineralogical, and
112 chemical processes within the models. Being highly dynamic in nature, K-factor rationalizes
113 the effect of various intrinsic soil properties on erosion (Wang et al., 2001). Environmental
114 Policy Integrated Climate (EPIC) Model (Williams et al., 1983) had been used by Godoi et al.,
115 (2021), to estimate soil erodibility factors across Brazil.

116 As discussed, empirical equations and models are widely used globally to assess the sensitivity
117 of model outputs to field-based erodibility factor values. However, due to the nature of data
118 inclusion and availability for the study location, it is imperative to look beyond a single
119 equation or model globally to capture impact of model variability on soil erodibility estimates.
120 The global research community now focuses on building composite models that might
121 replicate the field-based soil erodibility variables with greater accuracy. RUSLE's Nomograph
122 with other models like EPIC and erodibility indices had been estimated at the watershed or
123 regional scale across the world. In this research, the applicability of these models and indices
124 have been thoroughly assessed over the study region.

125 In India, pedological datasets are either unavailable at a national scale or are dispersed between
126 various research institutes and public agencies. Such problems compel researchers and
127 scientists to adopt empirical equations to estimate soil erodibility factor (Adhikary et al., 2014;
128 Mhaske et al., 2021; Olaniya et al., 2020; Paparrizos et al., 2015; Rozos et al., 2013). Very few
129 studies have been performed over the Indian region to calculate K-factors using field
130 observations (Adhikary et al., 2014; Bera, 2017; Olaniya et al., 2020). Adhikary et al., (2014)
131 estimated K-factors for Bundelkhand regions in Central India using four different empirical
132 models.

133 Olaniya et al., (2020) estimated soil erodibility and erodibility indices over Ri-Bhoi district of
134 Meghalaya. In absence of actual K-factor values, erodibility indices such as Clay Ratio (CR)
135 (Bennett, 1926), Modified Clay Ratio (MCR) (Kumar et al., 1995), and Critical Level of Soil

136 Organic Matter (CLOM) (Pieri, 2012) indices have been used to estimate soil erodibility. Soil
137 erodibility factors for Europe, mapped by Panagos et al., (2014) has been incorporated by many
138 scientists and researchers as input forcing data for their soil erosion models in Europe.
139 Estimation of soil erodibility over India thus remains a significant milestone required to
140 develop policy and tools useful for developing soil conservation and erosion mitigation plans.
141 In this study, we estimated soil erodibility factors over national scale using RUSLE
142 Nomograph (K_{NOMO}) and EPIC (K_{EPIC}) models. A detailed statistical evaluation of soil
143 erodibility map was also performed to visualize its distribution over the national region based
144 on soil types, texture, and percentage-range of erodibility values. Erodibility indices like CR,
145 MCR, and CLOM indices were estimated over India and its sensitivity with soil erodibility
146 was also checked. The soil erodibility index which was correlating K-factor with better
147 accuracy was plotted in scatter manner as well. CLOM index generally refers to the critical
148 availability of the organic carbon in soil, higher CLOM ratio suggests less susceptibility to soil
149 erosion. A susceptibility to soil erosion map was finally developed over India using CLOM
150 index classification. This study will provide a comprehensive understanding of the soil
151 erodibility factor and its indices over India and provide an additional K-factor dataset to
152 perform soil loss estimations over the national scale.

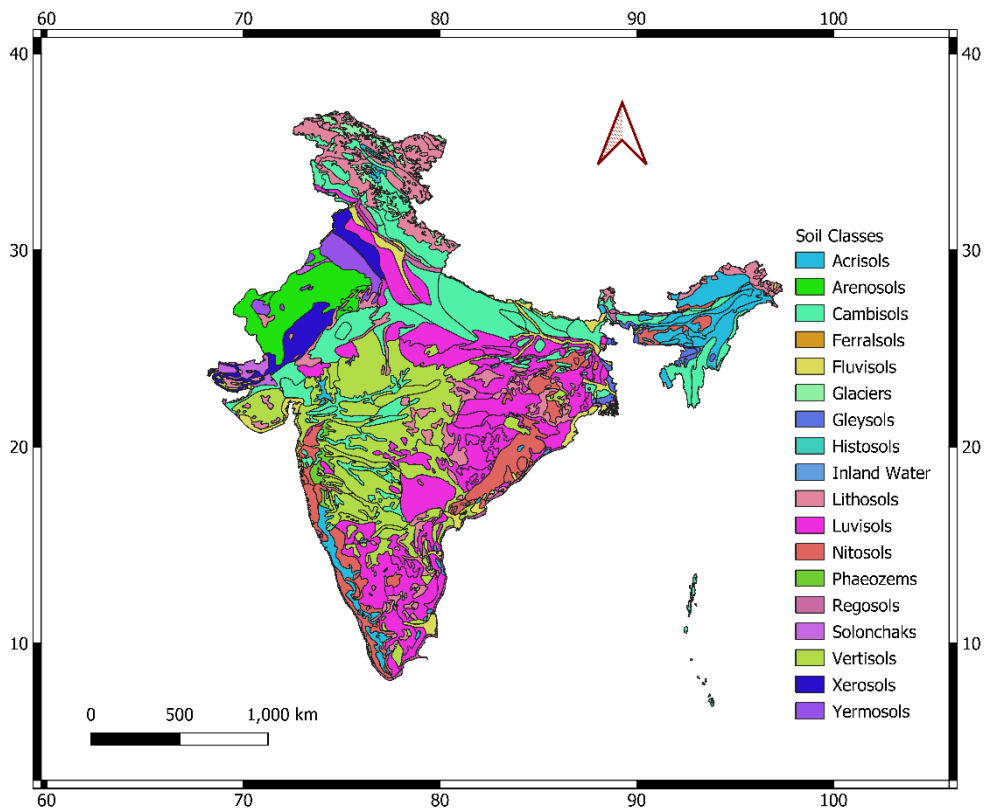
153 **2. Materials and Methodology**

154 **2.1 Study Area**

155 This study covers the political boundary of India, with an area equal to 36,57,948 km² between
156 68°7' - 97°25' and 8°4' - 37°6' longitude and latitude respectively. As the seventh largest nation
157 in the world by geographical area, an immense diversity distribution of soil types and
158 properties associated with it is observed throughout the country. A total of 18 classes of soils
159 are present according to the FAO-UNESCO (Food and Agriculture Organization – United
160 Nations Educational, Scientific and Cultural Organization) Soil Map of the World, which has
161 been shown in Figure 1.

162

163



164

165 **Figure 1.** Soil classes of India (Source: FAO-UNESCO Soil Map of the World)

166 Lithosols soil covers the maximum area (24.14%) while Ferralsols soil in minimum area
167 (0.02%) of the total land of the country. About 70% of the total land area of the nation is

168 covered by only four classes of soils (Lithosols (24.14%), Cambisols (16.93%), Luvisols
169 (16.12%) and Vertisols (13.12%)). Rest of the 14 soil classes (Acrisols, Arenosols, Ferralsols,
170 Fluvisols, Glaciers, Gleysols, Histosols, Nitosols, Phaeozems, Regosols, Solonchaks,
171 Xerosols, Yermosols, and Inland water) acquire only 30% of the total soil surface of the study
172 area. Considering the texture classes, as per the record of NBSS&LUP (National Bureau of
173 Soil Survey and Land Use Planning) India, about 45.12% of the total spread area of the nation
174 is loamy in nature, while 33.14% clayey and 11.17% sandy. About 7.56% of the total area
175 consists of Glaciers and Rock outcrops, 1.62% water bodies, 0.67% Rock mountains, and about
176 0.64% area covers the Rann of Kachchh.

177 2.2 *Data acquisition and preparation*

178 For estimating soil erodibility factor (K-factor) and the erodibility indices {Clay Ratio (CR),
179 Modified Clay Ratio (MCR), and Critical Level Organic Matter (CLOM)} over India, gridded
180 datasets associated with soil particle properties have been utilized. The datasets required were
181 percentage of sand, silt, clay, soil organic carbon (SOC), soil organic matter, soil texture class,
182 soil structure code (SSC), and soil permeability code (SPC). Percentage of sand, silt, clay, and
183 SOC were downloaded from SoilGrids of ISRIC (International Soil Reference and Information
184 Centre) (<https://soilgrids.org/>) (Hengl et al., 2017). Texture classes were prepared using
185 percentages of soil particles size data utilizing Soil Texture Calculator Triangle from NRCS
186 (Natural Resources Conservation Service) Soils – USDA (United States Department of
187 Agriculture). SSC and SPC were mapped using the prepared soil texture and soil groups
188 information at national scale.

189 2.2.1 *Soil particles properties*

190 SoilGrids is a platform where soil profile datasets are compiled using machine learning
191 methods to produce digital soil map over the globe. Global soil profile datasets are available
192 at WoSIS (World Soil Information Service). More than 230000 soil profiles, and a series of

193 environmental covariates are used to fit the SoilGrids prediction models. Various datasets
 194 associated with soil parameters are available on SoilGrids website. In this research, properties
 195 of soil particles such as content of silt, sand, clay, and soil organic carbon (SOC) had been
 196 used. These datasets were downloaded using Google Earth Engine (GEE) at 250 m resolution
 197 for entire India. The units of contents of sand, clay and silt are same i.e., weight percentage
 198 (g/g), but the unit of SOC is in g/kg. Soil organic matter (SOM) were also used in this study.
 199 Since the exact available organic matter data was unavailable, a conversion factor equal to 2
 200 was adopted in this research to convert SOC to SOM (Pribyl, 2010). Data of very fine fraction
 201 of sand was also not available at national scale, so a factor of 0.02 (20%) to the percentage
 202 content of sand particles was adopted based on Panagos et al. (2014).

203 2.2.2 Soil Texture Class

204 Natural Resources Conservation Service Soils (NRCS) of United States Department of
 205 Agriculture (USDA) has suggested the soil texture calculator triangle to calculate texture
 206 classes. Ranges of texture classes have been retrieved using the triangle which is shown in
 207 Table 1. In this classification system, the contents of sand, silt and clay have been considered
 208 to assign a texture class. Using this concept, texture classes (Sand, silt, clay, sandy loam, loamy
 209 sand, loam, silt loam, sandy clay loam, clay loam, sandy clay, silty clay loam, clay, and silty
 210 clay) were mapped throughout the nation.

211 **Table 1.** Ranges of contents of sand, silt, and clay for texture classification (NRCS-USDA)

Texture Class	Sand %	Silt %	Clay %
Sand	85-100	0-15	0-10
Sandy loam	43-85	0-50	0-20
Loamy sand	70-90	0-30	0-15
Loam	23-52	28-50	7- 27
Silt loam	0-50	50-88	0-27
Sandy Clay Loam	45-80	0-28	20-35
Clay Loam	20-45	15-53	27-40
Sandy Clay	45-60	0-20	35-55
Silty Clay loam	0-20	40-73	27-40
Clay	0-45	0-40	40-100

Silty Clay	0-20	40-60	40-60
Silt	0-20	80-100	0-12

212

213 *2.2.3 Soil Structure and Permeability Class*

214 Soil texture classes prepared using NRCS-USDA classification were further processed to
 215 assign texture and permeability classes over India. Sand texture class is generally blocky, platy,
 216 or massive in nature. Medium or coarse granular soil particles cover sandy loam, loamy sand,
 217 loam, silt loam, sandy clay loam, clay loam, sandy clay, and silty clay loam; while fine granular
 218 soils cover clay, silty clay and silt (Morgan, 2001). Structure and permeability classes were
 219 classified and shown in Table 2.

220 **Table 2.** Soil structure and permeability classes based on texture class (Efthimiou, 2020;
 221 Morgan, 2001)

Texture Class	Soil	Structure	Permeability
Sand	Blocky, Platy or Massive	4	1
Sandy loam	Medium or coarse granular	3	2
Loamy sand	Medium or coarse granular	3	2
Loam	Medium or coarse granular	3	3
Silt loam	Medium or coarse granular	3	3
Sandy Clay Loam	Medium or coarse granular	3	4
Clay Loam	Medium or coarse granular	3	4
Sandy Clay	Medium or coarse granular	3	5
Silty Clay loam	Medium or coarse granular	3	5
Clay	Fine granular	2	6
Silty Clay	Fine granular	2	6
Silt	Fine granular	2	6

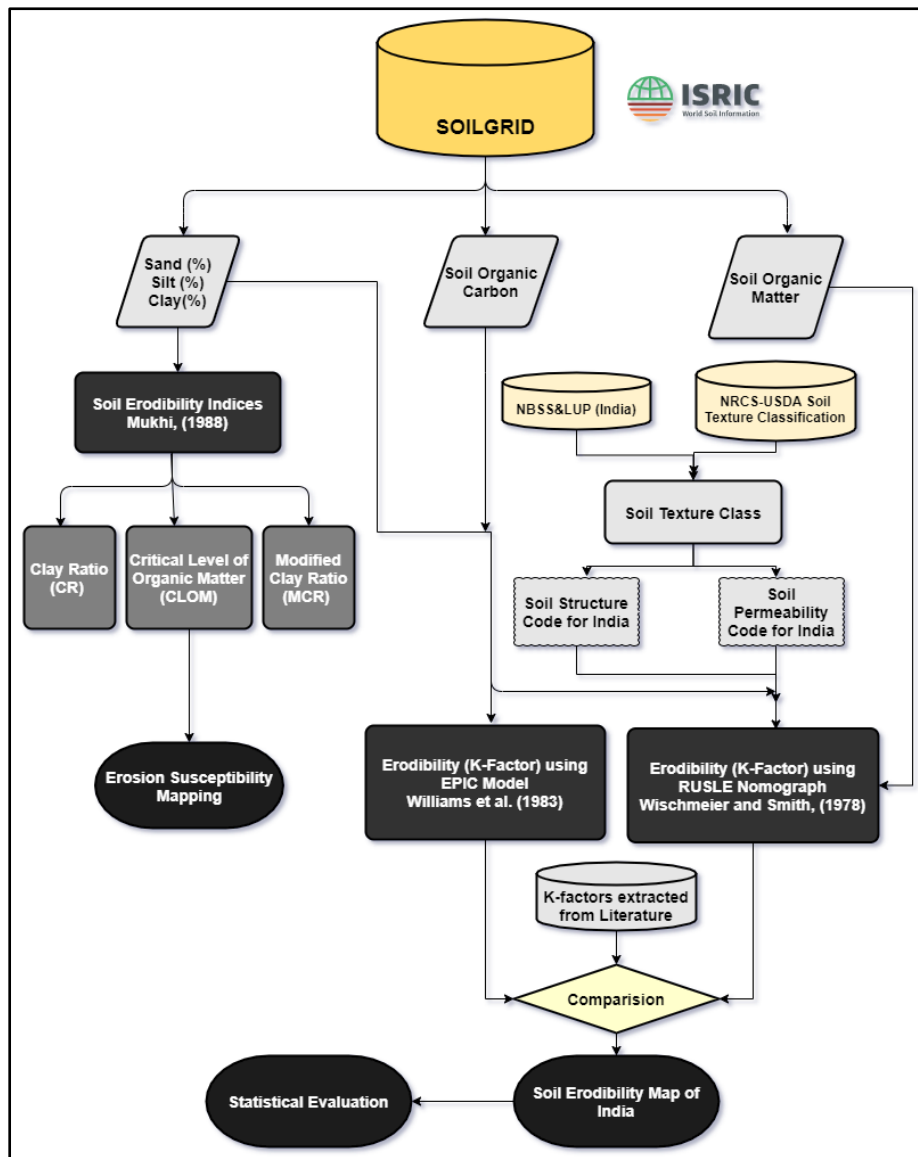
222

223

224 2.3 *Methodology*

225 Soil erodibility factors over India were mapped using two approaches – empirical methods and
226 indices. In the first method, soil erodibility factors were estimated using two widely used
227 models i.e., RUSLE Nomograph (K_{NOMO}) and EPIC Model (K_{EPIC}); while in the second
228 method, soil erodibility indices such as clay ratio (CR), modified clay ratio (MCR), and critical
229 level of organic matter (CLOM) were calculated. The complete methodology followed for the
230 soil erodibility mapping is given in Figure 2. Soil texture classes were prepared using NRCS-
231 USDA soil texture triangle (NRCS, 2016). Soil structure and permeability codes were also
232 mapped over the study area the prepared texture class with the help of the concept suggested
233 by Morgan (2001).

234



235

236 **Figure 2.** Workflow methodology for soil erodibility mapping over India

237 Further, a comparative analysis was also performed among the soil erodibility factors (K_{NOMO}
 238 and K_{EPIC}) and erodibility indices (CR, MCR and CLOM) to check the correlation. K-factor
 239 maps were compared with past studies in India. A detailed statical analysis of the soil
 240 erodibility map was also conducted to illustrate its distribution over the national region based
 241 on soil types, texture, and percentage-range erodibility values. A susceptibility map due to soil
 242 erosion was also prepared using the CLOM index values with the help of the concept suggested
 243 by Pieri, (2012). Arcmap 10.5, Google Earth Engine, Q-GIS 3.16, and Python libraries in
 244 Jupyter Notebook had been used to process and visualize the data.

245 2.3.1 Soil Erodibility Factor (*K*-factor)

246 Soil erodibility is a function of the content of sand, silt, clay, percentage of soil organic matter
 247 (SOM), permeability, and structure code (Renard et al., 1997; Wischmeier and Smith, 1978);
 248 and can be expressed as Equation 1.

$$249 K_{NOMO} = 0.1317\{(2.1 M^{1.14} * 10^{-4} * (12 - SOM) + 3.25 (s - 2) + 2.5 (p - 3)) \div 100\}$$

250 (Eq. 1)

251 Where: K_{NOMO} = Soil erodibility factor using Nomograph approach in t-ha-h/ha/MJ/mm

252 $M = \{(\% \text{ of silt} + \% \text{ of very fine sand}) * (100 - \% \text{ of clay})\} = \text{Particle size parameter}$

253 $SOM = \text{Percentage of soil organic matter}$

254 $s = \text{Soil structure code}$

255 $p = \text{Soil permeability code}$

256 The multiplication factor 0.1317, converts the unit of *K*-factor into SI unit i.e., t-ha-
 257 h/ha/MJ/mm. Percentage of very fine sand (vfs) was calculated as 20% of content of sand.
 258 Nomograph equation was defined for those types of soil profile where silt content is not more
 259 than 70%.

260 Williams et al., (1983) developed a model named EPIC (Environmental Policy Integrated
 261 Climate) to determine the relationship between soil productivity and soil erosion. The
 262 components of the model also include hydrology, tillage science, plant growth, nutrient
 263 dynamics, soil temperature, and economics. There were various physical components included
 264 in this model to describe the soil productivity and erosion phenomena. Soil erodibility factor
 265 using EPIC model approach (K_{EPIC}) is dependent on percentage of soil particle size (sand, silt,
 266 and clay) and soil organic carbon (SOC) only, expressed as shown in Equation 2.

$$267 K_{EPIC} = 0.1317 \left(0.2 + 0.3 * e^{\left(-0.0256 * SAND \left(1 - \left(\frac{SILT}{100} \right) \right) \right)} * \left(\frac{SILT}{CLAY + SILT} \right)^{0.3} * \left(1 - \left(0.25 * \right. \right. \right.$$

$$268 \left. \left. \frac{SOC}{SOC + e^{(3.72 - 2.95 * SOC)}} \right) \right) * \left(1 - \left(0.7 * \frac{SN}{SN + e^{(-5.51 + 22.9 * SN)}} \right) \right) \quad (\text{Eq. 2})$$

269

270 Where: K_{EPIC} = Soil erodibility factor in t-ha-h/MJ/ha/mm

271 $CLAY$ = % of clay content

272 $SILT$ = % of silt content

273 $SAND$ = % of sand content

274 SOC = % of soil organic carbon

275 $SN = \{1 - (SAND/100)\}$

276 The multiplication factor 0.1317, converts the unit of K-factor into SI unit i.e., t-ha-
277 h/ha/MJ/mm. Input data for K_{EPIC} was derived from SoilGrids up to depth of 30 cm from top.

278 2.3.2 *Erodibility Indices*

279 In the second method, to estimate soil erodibility factor erodibility indices like CR, MCR and
280 CLOM were calculated over India. Clay ratio (CR) is the property of soil by which binds the
281 soil particles tightly. Higher the number of clay particles, higher the clay ratio, and harder it is
282 to detach the soil particles by external forces (Bouyoucos, 1935). Clay ratio is inversely
283 proportional to K-factor. Clay ratio was further modified by introducing content of soil organic
284 matter (SOM) into it, and termed as modified clay ratio (MCR) (Mukhi, 1988; Tarafdar and
285 Ray, 2005). The clay ratio and modified clay ratio are shown in Equation 3 and Equation 4
286 simultaneously.

$$287 \quad CR = \left\{ \frac{(\%SAND + \%SILT)}{\%CLAY} \right\} \quad (\text{Eq. 3})$$

$$288 \quad MCR = \left\{ \frac{(\%SAND + \%SILT)}{(\%CLAY + \%SOM)} \right\} \quad (\text{Eq. 4})$$

289 Where: % (SAND, SILT, CLAY, SOM) = % of sand, silt, clay, and soil organic carbon.

290 Further, CLOM is also an index for soil erodibility and indicates the susceptibility caused due
291 to soil erosion (Pieri, 2012). It refers to the relative content of the soil organic matter (SOM)
292 available in the soil samples and expressed as shown in Equation 5.

293
$$CLOM = \left(\frac{SOM}{CLAY+SILT} \right) \quad (Eq.5)$$

294 Where: CLOM = Critical level of Organic matter

295 SOM, SILT and CLAY = Percentages of soil organic matter, silt, and clay content.

296 Lower values of CLOM refer to the higher susceptibility due to erosion. A detailed description
 297 of CLOM values with respect to susceptibility due to soil erosion is shown in Table 3. A
 298 susceptibility map due to soil erosion had been mapped over India using the classification
 299 concept given in Table 3 which is based on the percentage occurrence of the critical level of
 300 organic matter. Availability of organic matters in the soil provide strength against soil erosion
 301 it implies that lower the CLOM values, the greater the vulnerability to soil erosion. Best
 302 correlated erodibility index was also plotted against K-factor to visualize its variation
 303 corresponding to soil texture classes defined by NBSS & LUP, India.

304 **Table 3.** Classification of CLOM values for susceptibility due to erosion (Pieri, 2012)

Sr No	CLOM (%)	Susceptibility to Soil Erosion
1	(<5)	High
2	(5-7)	Moderate
3	(7-9)	Low
4	(>9)	Stable

305

306 .

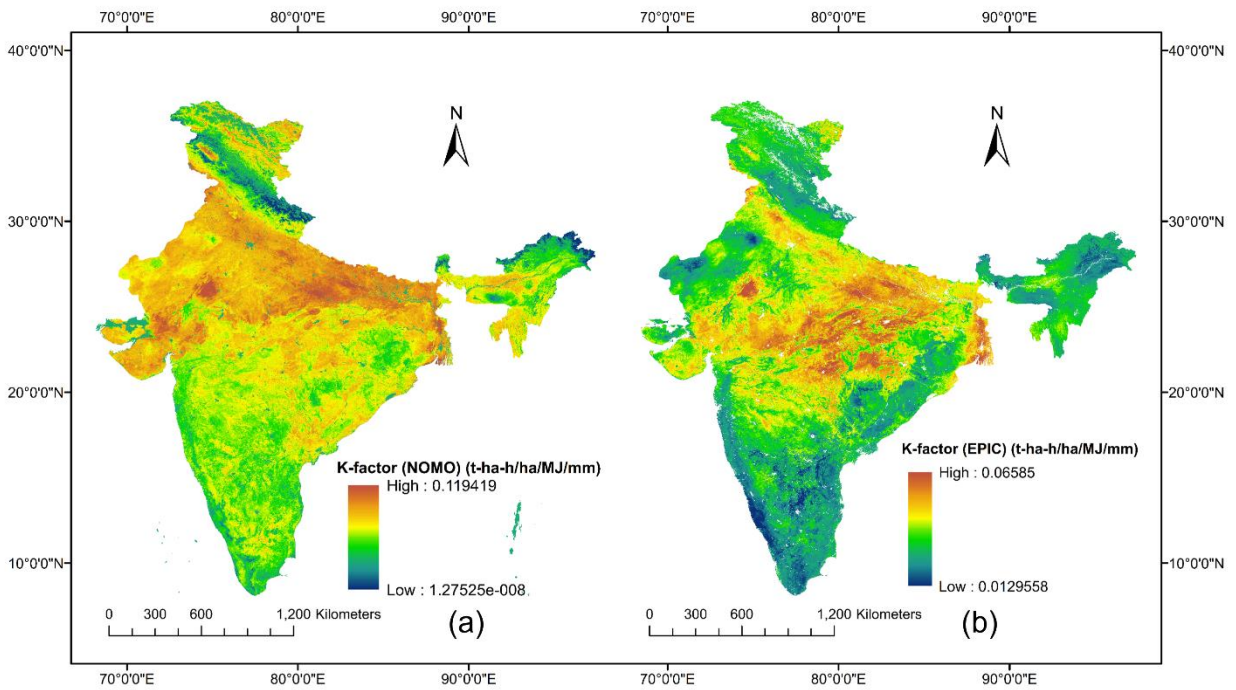
307 **3. Results and Discussions**

308 *3.1 Erodibility Factors*

309 Soil particle parameters (percentage of sand, silt, clay, structure code, permeability code, SOC,
 310 SOM, and vfs) had been used to estimate K-factors using Nomograph and EPIC model
 311 approaches. Soil erodibility factor maps (K_{NOMO} and K_{EPIC}) have been shown in Figures 3 (a)
 312 and (b) respectively. The national average soil erodibility value for India was calculated as
 313 0.028 and 0.034 t-ha-h/ha/MJ/mm using Nomograph and EPIC model approaches respectively.
 314 A detailed statistics of K-factors has been shown in Table 4.

315

316



317

318 **Figure 3. (a) and (b)** Soil erodibility factor maps (K_{NOMO} and K_{NOMO}) over India using
 319 RUSLE Nomograph and EPIC models respectively

320 **Table 4.** Statistical summary of erodibility factors and indices K-factor

Parameters	Minimum	Maximum	Average	Standard Deviation
K-EPIC	0.013	0.065	0.034	0.004
K-NOMO	$1.27 * 10^{(-8)}$	0.11	0.028	0.007
CR	0.77	10.776	2.32	0.85

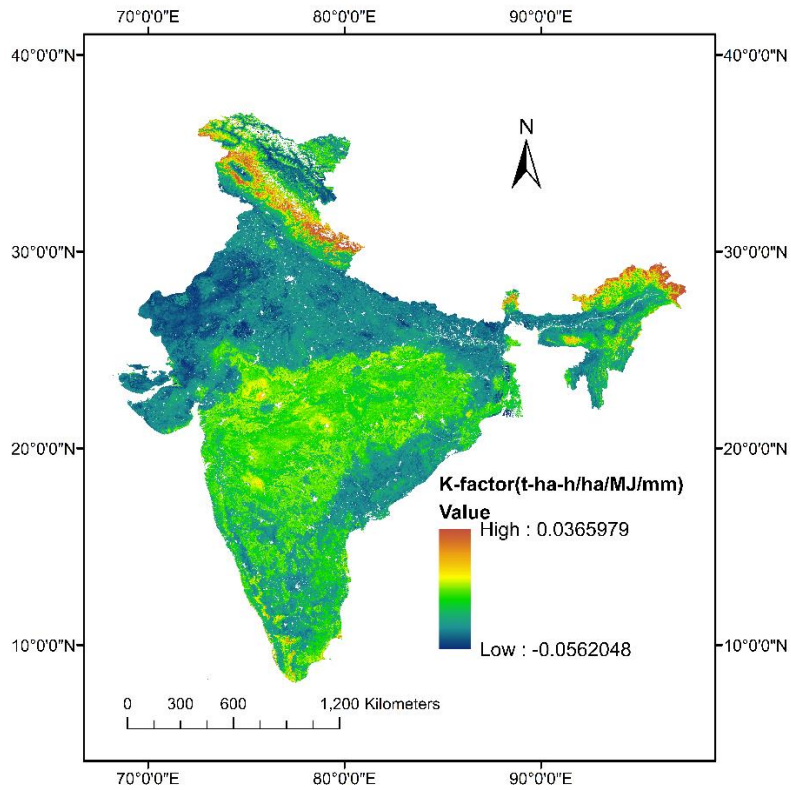
MCR	0.000	8.05	2.07	0.67
CLOM	0.000	24.1	2.96	2.222

321 The Nomograph approach for calculating K-factor allows the SOM less than or equal to 12 as
322 mentioned in Equation 1 with $\{(12 - \text{SOM})\}$ term. In this study, SOM values were estimated
323 in the range of 0 to 22.52%. The term associated with permeability code (p) in Equation 1 also
324 effected negatively by the permeability codes 1 and 2 which generally refer to the soil types
325 with blocky, platy, or massive, medium, or coarse granular soil particles. It was observed that
326 these factors were responsible to reflect negative values of K-factor using Nomograph method.
327 These negative values were only 0.22% of the total pixels in the study region. It was observed
328 that the negative values were ranged from 0 to -0.017 and occurred in the regions having soil
329 types with blocky, platy, or massive, medium, or coarse granular soil particles which have
330 higher resistivity to soil erosion. To rectify these negative values, the modulus of K-factor was
331 incorporated. Lower values of K-factor reflect higher resistivity against soil erosion.
332 Higher values of erodibility refer to the high susceptibility due to soil erosion in those regions
333 and vice versa (Kumar and Kushwaha, 2013). It was also observed that K-factors estimated
334 using EPIC model had been overestimated the soil erodibility values than that of Nomograph
335 model. A difference map had been created between K_{EPIC} and K_{NOMO} maps, which has been
336 shown in Figure 4. The difference K-factor values ranges from -0.025 to 0.035 t-ha-
337 h/ha/MJ/mm. This map was created by subtracting K_{NOMO} values from K_{EPIC} values, and it was
338 observed that about 85% values were overestimated using EPIC model. This could be due to
339 the parameters taken to estimate soil erodibility by both the models. EPIC model does not
340 count the structure and permeability codes while these two parameters are associated with the
341 Nomograph model and creates adequate impact on the soil erodibility estimated using this
342 model. Taking into account the structural and permeability factors of soil, it offers additional
343 information about the qualities of soil particles that is crucial for preventing soil erosion by
344 influencing soil erodibility values.

345

346

347



348

349 **Figure 4.** Difference map of K-factor estimated using EPIC model compared with Nomograph
350 model

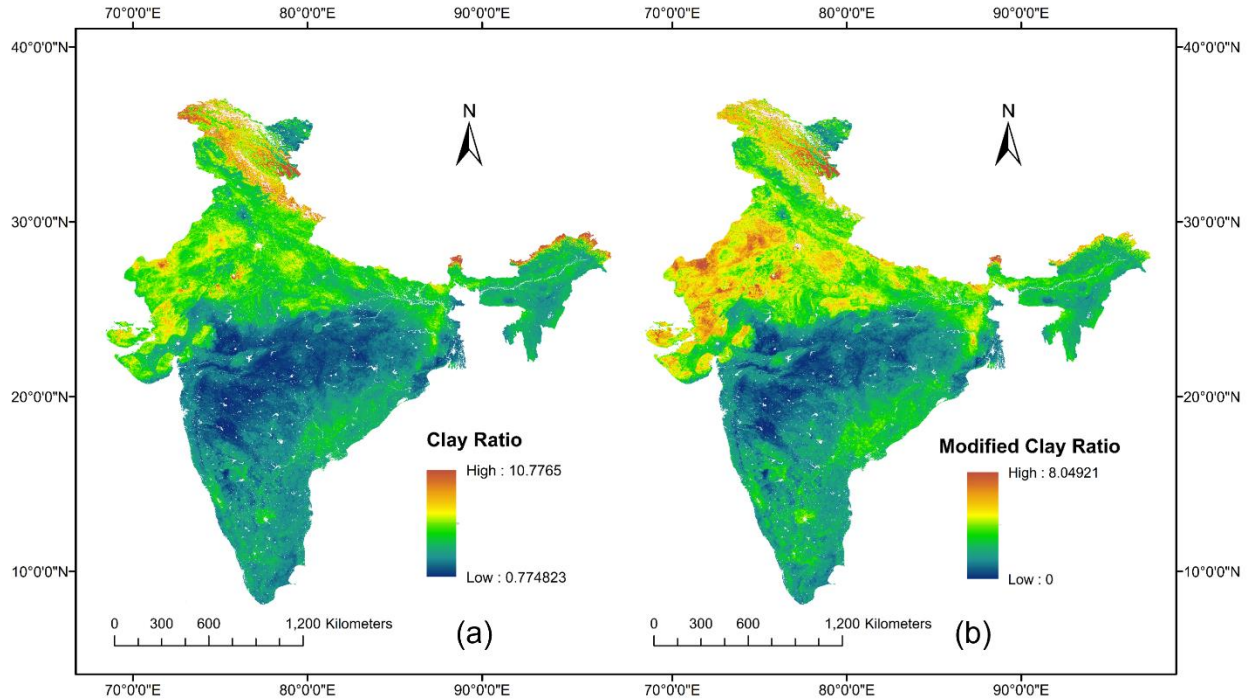
351 *3.2 Erodibility Indices*

352 Clay ratio (CR) and Modified Clay Ratio (MCR) were calculated using percentage content of
353 sand, silt, clay, and SOM present in the soil samples, which have been shown in Figures 5(a)
354 and (b). Average CR and MCR for India was calculated as 2.32 and 2.07, while maximum as
355 22.81 and 17.42 respectively. The differences in the spatial variation of these two indices could
356 be visualize in Figure 5(a) and (b) where higher values (>5) were spotted in the northern upper
357 side of the study region (Jammu and Kashmir, Himanchal Pradesh) and some portions of
358 Arunachal Pradesh, Punjab, and Sikkim states of India. These differences are due to the

359 consideration of organic matter availability in modified clay ratio which reduces the value of
360 MCR in comparison to CR.

361

362



363

364 **Figure 5. (a) and (b) Clay Ratio (CR) and Modified Clay Ratio (MCR) Maps over India**

365 Higher clay ratio suggests a greater potential to avoid soil erosion which means lower
366 susceptibility to soil erosion. Higher CR values were spotted in the border areas of Arunachal
367 Pradesh, Sikkim, Uttarakhand, Himanchal Pradesh, and a few regions of Rajasthan and Jammu
368 and Kashmir; while lower values were spotted in the regions of Central India (Figure 5 (a)).

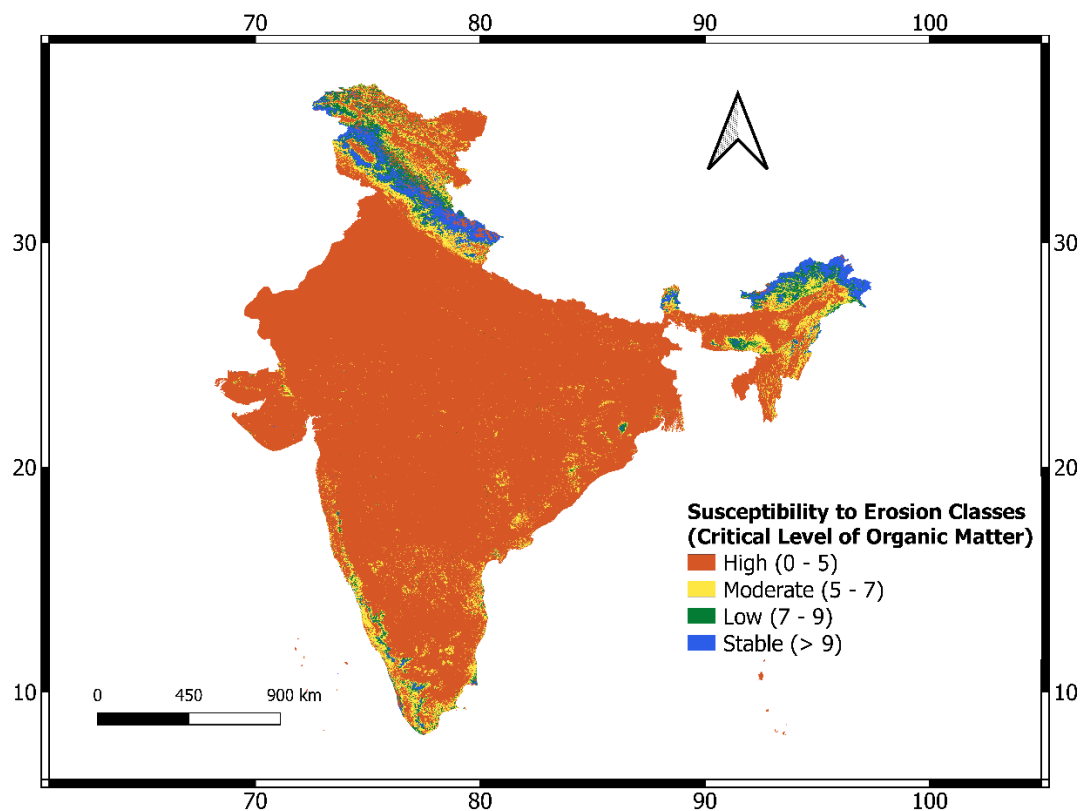
369 Apart from the regions covered by higher CR values, MCR also covered major portions of
370 Rajasthan, Gujarat, and some regions of Uttar Pradesh and Haryana having higher values which
371 referred to the low susceptibility due to soil erosion in these regions (Figure 5 (b)).

372 Critical level of organic matter (CLOM) ratio was calculated using the soil particles parameter
373 datasets over India which has been shown in Figure. 6. As indicated by the name itself, this
374 index refers to the availability of the relative content of SOM which suggests that higher

375 CLOM values are less susceptible to soil erosion. The CLOM map was further classified in
376 susceptibility classes due to soil erosion (Pieri, 2012) according to Table 3, which has been
377 shown in Figure 6. Only border areas of Arunachal Pradesh, Sikkim, Uttarakhand, Himanchal
378 Pradesh, and some regions of Jammu and Kashmir were identified as stable regions due to soil
379 erosion considering the higher CLOM values. Major portion of the country (>80%) areas were
380 spotted as high susceptible regions due to soil erosion having lower CLOM values.

381

382



383

384 **Figure 6.** Susceptibility to soil erosion classes based on Critical Level of Organic Matter
385 (CLOM) values

386 3.3 Relationship between K-factors and erodibility indices

387 Erodibility indices (CR, MCR and CLOM) had been used as an alternate approach to estimate
388 soil erodibility earlier. These indices were further compared with the K-factors estimated using
389 both models (K_{NOMO} and K_{EPIC}) in this study. Pearson's correlation coefficients were calculated

390 among erodibility indices and K-factors which is shown in Table 5. Erodibility factors
 391 computed using both the methods was giving a correlation coefficient of 0.64 despite showing
 392 overestimation in calculating K-factor by EPIC method. It was observed that only CR with
 393 MCR, and CLOM index with K_{NOMO} was correlating with better accuracy having Pearson's
 394 correlation equals to 0.95 and -0.73 respectively. Negative correlation shows that if the value
 395 of CLOM index increases, the values of K_{NOMO} decreases; and vice versa. Clay ratio was worst
 396 correlated with K-factors estimated using both methods having correlation coefficients 0.07
 397 and -0.17 because of the data requirements to calculate these parameters. Clay ratio only
 398 incorporates sand, silt, and clay percentages while Nomograph and EPIC models use soil
 399 particle parameters and content of SOC as additional input data. Best correlated erodibility
 400 (CLOM) index was further plotted against K-factor to visualize its variation corresponding to
 401 soil texture classes defined by NBSS & LUP, India which has been shown in Figure 7.

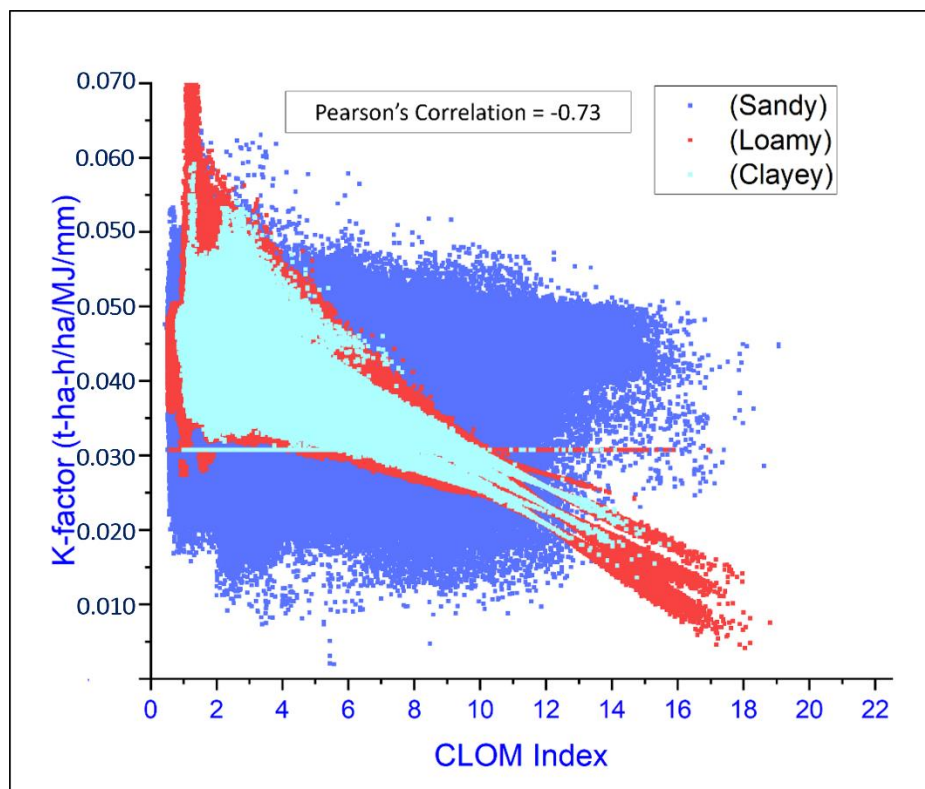
402 **Table 5.** Correlation coefficients among K-factors and erodibility indices

	CR	MCR	CLOM	K_{NOMO}	K_{EPIC}
CR	1	0.95	0.43	0.07	-0.17
MCR	0.95	1	0.15	0.33	-0.08
CLOM	0.43	0.17	1	-0.73	-0.52
K_{NOMO}	0.07	0.33	-0.73	1	0.64
K_{EPIC}	-0.17	-0.07	-0.52	0.64	1

403

404

405



406

407 **Figure 7.** Scatter plot between K-factors (t-ha-h/ha/MJ/mm) and Critical Level of Organic
 408 Matter (CLOM) index highlighting for major soil texture classes (Loamy, Clayey, and Sandy).

409 *3.4 Distribution of soil erodibility (K-factor)*

410 The average soil erodibility factors (K_{NOMO} and K_{EPIC}) for India are estimated as 0.028 and
 411 0.034 respectively. The soil types and texture classes are not uniform though out the nation
 412 leading to the spatial variability of K-factors in India. Both the K_{NOMO} and K_{EPIC} factors were
 413 compared with the few existing studies that have been conducted in India. Bera, (2017) had
 414 estimated soil erosion for Gumti river basin of Tripura, India, where he had also estimated soil
 415 erodibility values. Olaniya et al., (2020) also estimated K-factors for Ri-Bhoi district of
 416 Meghalaya, India. These two K-factors were collected by the authors, and a statical comparison
 417 (Minimum, maximum, and average) with the estimated K-factors has been shown in Table 6.
 418 The K-factor values mentioned in the literature were converted into the SI unit (t-ha-
 419 h/ha/MJ/mm) to compare with calculated K-factors using both the methods.

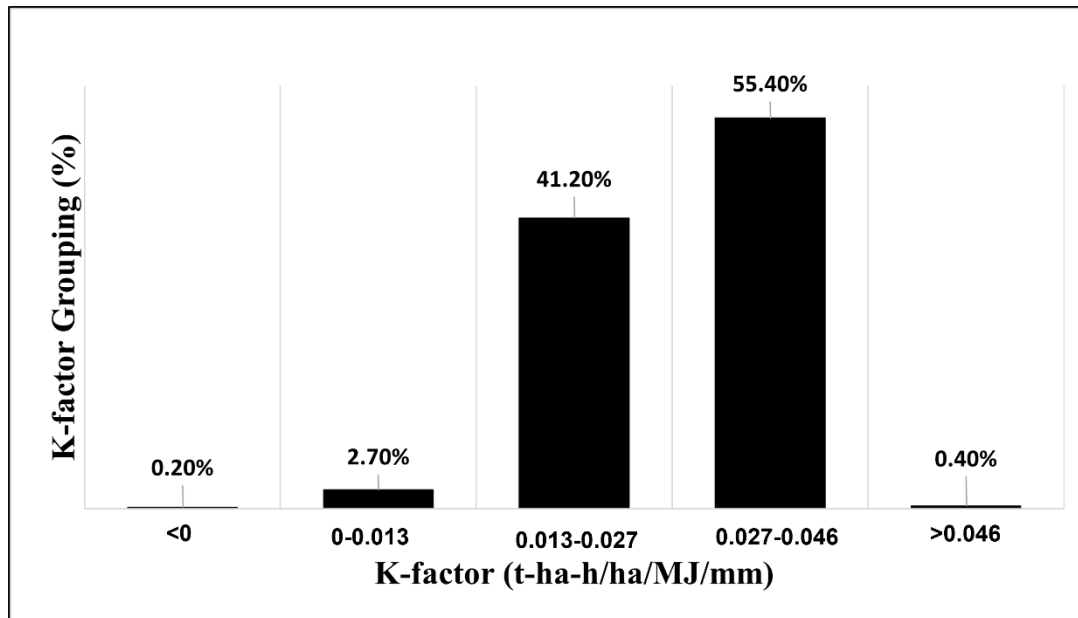
420 **Table 6.** Comparison of estimated K-factor values with the extracted K-factors from literature

	Gumti River Basin (Tripura, India)			Ri-Bhoi District (Meghalaya, India)		
	K _{NOMO}	K _{EPIC}	K-Literature	K _{NOMO}	K _{EPIC}	K-Literature
Minimum	0.014	0.029	0.012	0.014	0.026	0.011
Maximum	0.043	0.043	0.047	0.041	0.040	0.055
Average	0.030	0.034	0.035	0.026	0.029	0.029

421

422 By analyzing the values of K-factors from Table 6, it was observed that K_{NOMO} shows relatively
423 better relationship with the K-factors reported in the literature based on the minimum,
424 maximum, and average values. The erodibility factor was estimated in the range of (0 to 0.054
425 t-ha-h/ha/MJ/mm) (Godoi et al., 2021) for Brazil, (0.013 to 0.044 t-ha-h/ha/MJ/mm)
426 (Efthimiou, 2020) for Greece, (0.02 to 0.05 t-ha-h/ha/MJ/mm) (Bonilla and Johnson, 2012) for
427 Central Chile, (0.02 to 0.07 t-ha-h/ha/MJ/mm) (Yang et al., 2018) for New South Wales,
428 Australia, and (0.026 to 0.076 t-ha-h/ha/MJ/mm) (Panagos et al., 2014) for European countries.
429 Adhikary et al., (2014) had also mapped K-factors in Bundelkhand region of Central India
430 which covers thirteen districts of Madhya Pradesh and Uttar Pradesh using four models. The
431 average K-factors extracted from the research paper published by Adhikary et al., (2014) was
432 about 0.032 t-ha-h/ha/MJ/mm, which was matching with the average K-factor value (0.034 t-
433 ha-h/ha/MJ/mm) estimated by Nomograph approach (K_{NOMO}). This, for further mapping of the
434 distribution of K-factors throughout the national region, we adopted the K_{NOMO} values as the
435 standard. Total number of pixels available in the K-factor map of India, were grouped in five
436 ranges which has been shown in Figure 8. About 96.6% of the pixels of K-factors were spotted
437 in the range of (0.013-0.046) t-ha-h/ha/MJ/mm, while only 2.9% values were less than 0.013
438 t-ha-h/ha/MJ/mm, and 0.4% values of K-factor were recorded more than 0.0467 (t-ha-
439 h/ha/MJ/mm). About 55.8% of the K-factor values were greater than the national average K-
440 factor (0.028 t-ha-h/ha/MJ/mm).

441



442

443 **Figure 8.** Distribution of the range of K-factors (t-ha-h/ha/MJ/mm) grouped in percentages in
 444 the form of bar-chart

445 To make the study usable at the policy level, the K_{NOMO} map was used to extract average K-
 446 factor values for the soil classes defined by FAO-UNESCO. Considering the soil classes across
 447 the country, Histosols soil type was observed as least susceptible to soil erosion having lowest
 448 average K-factor (0.011 t-ha-h/ha/MJ/mm) while Xerosols soil type was most susceptible to
 449 soil erosion having highest average K-factor (0.034 t-ha-h/ha/MJ/mm) corresponding to the
 450 particular soil classes in Indian condition. These soil classes can be referred to Figure 1 for
 451 better visualization of the distribution of the soil classes. About 71% of the national spread
 452 area was spotted as average K-factor values greater than national average K-factor (0.028 t-
 453 ha-h/ha/MJ/mm) which covered eight (Vertisols, Luvisols, Gleysols, Fluvisols, Cambisols,
 454 Arenosols, Yermosols, and Xerosols) out of the eighteen soil classes.

455

456 **4. Conclusions and Future Work**

457 This study is an attempt to map soil erodibility and its distribution throughout the nation and
458 check the applicability of erodibility indices to estimate soil erodibility factor in the Indian
459 region. High resolution (250 m) input datasets for soil erodibility estimation from SoilGrids
460 had been downloaded and processed to get K-factor and erodibility indices over India. The
461 conclusions of this study are as follows:

- 462 • Using two widely adopted soil erodibility models (RUSLE Nomograph, and EPIC
463 Model), it is observed that K-factors estimated using Nomograph model (K_{NOMO})
464 shows better agreement with the past studies.
- 465 • National average soil erodibility factor for India were estimated as 0.028 and 0.034 t-
466 ha-h/ha/MJ/mm using Nomograph and EPIC models respectively.
- 467 • About 96.6% values of K-factors were spotted in the range of (0.013-0.046) t-ha-
468 h/ha/MJ/mm, while only 0.4% values of K-factor were recorded more than 0.046 (t-ha-
469 h/ha/MJ/mm). About 55.8% of the K-factor values were greater than the national
470 average K-factor (0.028 t-ha-h/ha/MJ/mm).
- 471 • Histosols soil type was observed as least susceptible to soil erosion having lowest
472 average K-factor (0.011 t-ha-h/ha/MJ/mm) while Xerosols soil type was most
473 susceptible to soil erosion having highest average K-factor (0.034 t-ha-h/ha/MJ/mm)
474 corresponding to the soil classes in Indian condition.
- 475 • Soil erodibility indices (CR, MCR, and CLOM index) had been also compared with
476 the K-factors (K_{NOMO} and K_{EPIC}) to check the relationships of these indices with K-
477 factor. It was observed that only CLOM index was showing better correlation
478 (Pearson's correlation = -0.73) with K_{NOMO} in Indian condition.
- 479 • A susceptibility to soil erosion map was also created based on CLOM index over India
480 and it was observed that only the border regions of Arunachal Pradesh, Sikkim,
481 Uttarakhand, Himachal Pradesh, and some regions of Jammu and Kashmir were spotted
482 as stable zones due to soil erosion.

483 This is the first national-scale mapping of soil erodibility factor over India which will be an
484 important asset for soil and erosion management planning by experts. This study will
485 complement the national mapping of rainfall erosivity (Raj et al., 2022) in an effort to develop
486 a systematic and comprehensive understanding of soil erosion over India. Since extensive local
487 ground measurements were not available for this study, global gridded datasets were utilized
488 instead. However, these datasets have their own limitations, depending on the statistical
489 approaches used to interpolate point spatial values of soil characteristics. To improve the
490 accuracy of soil erodibility factor estimates, future studies could benefit from the availability
491 of local ground-based observations at higher spatial resolutions. By incorporating more precise
492 and comprehensive data, we can overcome the limitations of global gridded datasets and obtain
493 more accurate estimates of soil erodibility. This will help in developing better soil conservation
494 and erosion management strategies that can effectively protect the soil and the environment.

495 **Acknowledgements:**

496 This research was conducted in the HydroSense Lab (<https://hydrosense.iitd.ac.in/>) at the
497 Indian Institute of Technology Delhi. This work was supported by an ISRO Space Technology
498 Cell grant (RP04139). This work was also supported by the IIT Delhi New Faculty Seed Grant.
499 The authors gratefully acknowledge the SoilGrids of ISRIC (International Soil Reference and
500 Information Centre) for providing access to the datasets. The authors would also like to thank
501 Dr. Amit Bera from the Department of Geography and Disaster Management, Tripura
502 University, India, and Dr. Manish Olaniya from the School of Natural Resource Management,
503 Central Agriculture University (Imphal), Meghalaya, India, for providing the field-based K-
504 factor results for validation. The authors would also like to thank the handling editor and the
505 anonymous reviewers for providing valuable comments, which significantly improved the
506 quality of this manuscript.

507 **Compliance with Ethical Standards**

508 The authors declare that they have no conflict of interest.

509 **Data Availability**

510 The dataset and shapefiles are available as ISED (Indian Soil Erodibility Dataset) with this
511 repository: <https://zenodo.org/record/6505511>

512

513 **References:**

- 514 Adhikary, P.P., Tiwari, S.P., Mandal, D., Lakaria, B.L., Madhu, M., 2014. Geospatial
515 comparison of four models to predict soil erodibility in a semi-arid region of Central
516 India. *Environ. Earth Sci.* 72, 5049–5062. <https://doi.org/10.1007/s12665-014-3374-7>
- 517 Balasubramani, K., Veena, M., Kumaraswamy, K., Saravanabavan, V., 2015. Estimation of
518 soil erosion in a semi-arid watershed of Tamil Nadu (India) using revised universal soil
519 loss equation (rusle) model through GIS. *Model. Earth Syst. Environ.* 1, 1–17.
- 520 Bennett, H.H., 1926. Some comparisons of the properties of humid-tropical and humid-
521 temperate American soils; with special reference to indicated relations between chemical
522 composition and physical properties. *Soil Sci.* 21, 349–376.
- 523 Bera, A., 2017. Assessment of soil loss by universal soil loss equation (USLE) model using
524 GIS techniques : a case study of Gumti River Basin ., *Model. Earth Syst. Environ.* 3, 1–
525 9. <https://doi.org/10.1007/s40808-017-0289-9>
- 526 Bhattacharyya, R., Ghosh, B.N., Mishra, P.K., Mandal, B., Rao, C.S., Sarkar, D., Das, K.,
527 Anil, K.S., Lalitha, M., Hati, K.M., 2015. Soil degradation in India: Challenges and
528 potential solutions. *Sustainability* 7, 3528–3570.
- 529 Bonilla, C.A., Johnson, O.I., 2012. Soil erodibility mapping and its correlation with soil
530 properties in Central Chile. *Geoderma* 189–190, 116–123.
531 <https://doi.org/10.1016/j.geoderma.2012.05.005>
- 532 Borrelli, P., Robinson, D.A., Panagos, P., Lugato, E., Yang, J.E., Alewell, C., Wuepper, D.,
533 Montanarella, L., Ballabio, C., 2020. Land use and climate change impacts on global soil
534 erosion by water (2015-2070). *Proc. Natl. Acad. Sci.* 117, 21994–22001.
- 535 Bouyoucos, G.J., 1935. Clay ratio as a criterion of susceptibility of soils to erosion. *J. Am.*
536 *Soc. Agron.*
- 537 Chen, X., Zhou, J., 2013. Volume-based soil particle fractal relation with soil erodibility in a
538 small watershed of purple soil. *Environ. earth Sci.* 70, 1735–1746.
- 539 Choudhury, B.U., Ansari, M.A., Chakraborty, M., Meetei, T.T., 2021. Effect of land-use
540 change along altitudinal gradients on soil micronutrients in the mountain ecosystem of
541 Indian (Eastern) Himalaya. *Sci. Rep.* 11, 1–13.
- 542 Cohen, M.J., Shepherd, K.D., Walsh, M.G., 2005. Empirical reformulation of the universal
543 soil loss equation for erosion risk assessment in a tropical watershed. *Geoderma* 124,
544 235–252.
- 545 Dangler, E.W., El-Swaify, S.A., 1976. Erosion of selected Hawaii soils by simulated rainfall.

546 Soil Sci. Soc. Am. J. 40, 769–773.

547 Efthimiou, N., 2020. The new assessment of soil erodibility in Greece. *Soil Tillage Res.* 204,
548 104720. <https://doi.org/10.1016/j.still.2020.104720>

549 Flanagan, D.C., Frankenberger, J.R., Ascough II, J.C., 2012. WEPP: Model use, calibration,
550 and validation. *Trans. ASABE* 55, 1463–1477.

551 Ghosh, B.N., Dogra, P., Sharma, N.K., Dadhwal, K.S., 2012. Soil erosion-productivity
552 relationship assessment in sloping lands of north-west Himalayas. *Indian J Agric Sci* 82,
553 1068–1071.

554 Godoi, R. de F., Rodrigues, D.B.B., Borrelli, P., Oliveira, P.T.S., 2021. High-resolution soil
555 erodibility map of Brazil. *Sci. Total Environ.* 781, 146673.
556 <https://doi.org/10.1016/j.scitotenv.2021.146673>

557 Guo, Y., Peng, C., Zhu, Q., Wang, M., Wang, H., Peng, S., He, H., 2019. Modelling the
558 impacts of climate and land use changes on soil water erosion: Model applications,
559 limitations and future challenges. *J. Environ. Manage.* 250, 109403.
560 <https://doi.org/10.1016/j.jenvman.2019.109403>

561 Hengl, T., Mendes de Jesus, J., Heuvelink, G.B.M., Ruiperez Gonzalez, M., Kilibarda, M.,
562 Blagotić, A., Shangguan, W., Wright, M.N., Geng, X., Bauer-Marschallinger, B., 2017.
563 SoilGrids250m: Global gridded soil information based on machine learning. *PLoS One*
564 12, e0169748.

565 Jiang, C., Zhang, H., Zhang, Z., Wang, D., 2019. Model-based assessment soil loss by wind
566 and water erosion in China's Loess Plateau: Dynamic change, conservation
567 effectiveness, and strategies for sustainable restoration. *Glob. Planet. Change* 172, 396–
568 413.

569 Kazamias, A.P., Sapountzis, M., 2017. Spatial and temporal assessment of potential soil
570 erosion over Greece 315–321.

571 Kulimushi, L.C., Maniragaba, A., Choudhari, P., Elbeltagi, A., Uwemeye, J., Rushema, E.,
572 Singh, S.K., 2021. Evaluation of soil erosion and sediment yield spatio-temporal pattern
573 during 1990–2019. *Geomatics, Nat. Hazards Risk* 12, 2676–2707.
574 <https://doi.org/10.1080/19475705.2021.1973118>

575 Kumar, K., Tripathi, S.K., Bhatia, K.S., 1995. Erodibility characteristics of Rendhar
576 watershed soils of Bundelkhand. *Indian J. Soil Conserv.* 23, 200–204.

577 Kumar, N., Singh, S.K., 2021. Soil erosion assessment using earth observation data in a trans-
578 boundary river basin. *Nat. Hazards* 107, 1–34.

579 Kumar, S., Kushwaha, S.P.S., 2013. Modelling soil erosion risk based on RUSLE-3D using

580 GIS in a Shivalik sub-watershed. *J. Earth Syst. Sci.* 122, 389–398.
581 <https://doi.org/10.1007/s12040-013-0276-0>

582 Lobo, G.P., Bonilla, C.A., 2019. Predicting soil loss and sediment characteristics at the plot
583 and field scales: Model description and first verifications. *Catena* 172, 113–124.

584 Lu, D., Li, G., Valladares, G.S., Batistella, M., 2004. Mapping soil erosion risk in Rondonia,
585 Brazilian Amazonia: using RUSLE, remote sensing and GIS. *L. Degrad. Dev.* 15, 499–
586 512.

587 Ma, J.W., Xue, Y., Ma, C.F., Wang, Z.G., 2003. A data fusion approach for soil erosion
588 monitoring in the Upper Yangtze River Basin of China based on Universal Soil Loss
589 Equation (USLE) model. *Int. J. Remote Sens.* 24, 4777–4789.

590 Mhaske, S.N., Pathak, K., Dash, S.S., Nayak, D.B., 2021. Assessment and management of
591 soil erosion in the hilltop mining dominated catchment using GIS integrated RUSLE
592 model. *J. Environ. Manage.* 294, 112987. <https://doi.org/10.1016/j.jenvman.2021.112987>

593 Morgan, R.P.C., 2001. A simple approach to soil loss prediction: a revised Morgan–Morgan–
594 Finney model. *Catena* 44, 305–322.

595 Mukhi, A.K., 1988. Erodibility of some vertisols. *J. Indian Soc. Soil Sci.* 36, 532–536.

596 Nearing, M.A., Foster, G.R., Lane, L.J., Finkner, S.C., 1989. A process-based soil erosion
597 model for USDA-Water Erosion Prediction Project technology. *Trans. ASAE* 32, 1587–
598 1593.

599 Nearing, M.A., Jetten, V., Baffaut, C., Cerdan, O., Couturier, A., Hernandez, M., Le
600 Bissonnais, Y., Nichols, M.H., Nunes, J.P., Renschler, C.S., 2005. Modeling response of
601 soil erosion and runoff to changes in precipitation and cover. *Catena* 61, 131–154.

602 NRCS, U., 2016. Soil texture calculator.

603 Olaniya, M., Bora, P.K., Das, S., Chanu, P.H., 2020. Soil erodibility indices under different
604 land uses in Ri-Bhoi district of Meghalaya (India). *Sci. Rep.* 10, 1–13.
605 <https://doi.org/10.1038/s41598-020-72070-y>

606 Panagos, P., Meusburger, K., Ballabio, C., Borrelli, P., Alewell, C., 2014. Soil erodibility in
607 Europe: A high-resolution dataset based on LUCAS. *Sci. Total Environ.* 479, 189–200.

608 Paparrizos, S., Maris, F., Kitikidou, K., Anastasiou, T., Potouridis, S., 2015. Comparative
609 analysis of soil erosion sensitivity using various quantizations within GIS environment:
610 an application on Sperchios river basin in Central Greece. *Int. J. river basin Manag.* 13,
611 475–486.

612 Pieri, C.J.M.G., 2012. Fertility of soils: A future for farming in the West African savannah.
613 Springer Science & Business Media.

614 Pribyl, D.W., 2010. A critical review of the conventional SOC to SOM conversion factor.
615 *Geoderma* 156, 75–83.

616 Raj, R., Saharia, M., Chakma, S., Rafieinasab, A., 2022. Mapping rainfall erosivity over India
617 using multiple precipitation datasets. *Catena* 214, 106256.
618 <https://doi.org/10.1016/j.catena.2022.106256>

619 Renard, K.G., Foster, G.R., Weesies, G.A., McCool, D.K., Yoder, D.C., 1997. Predicting Soil
620 Erosion by Water: A Guide to Conservation Planning With the Revised Universal Soil
621 Loss Equation (RUSLE), U.S. Department of Agriculture, Agriculture Handbook No.
622 703.

623 Renard, K.G., Foster, G.R., Weesies, G.A., Porter, J.P., 1991. RUSLE: revised universal soil
624 loss equation. *J. Soil Water Conserv.* 46, 30–33.

625 Rozos, D., Skilodimou, H.D., Loupasakis, C., Bathrellos, G.D., 2013. Application of the
626 revised universal soil loss equation model on landslide prevention. An example from N.
627 Euboea (Evia) Island, Greece. *Environ. Earth Sci.* 70, 3255–3266.

628 Saghafian, B., Meghdadi, A.R., Sima, S., 2015. Application of the WEPP Model to Determine
629 Sources of Run-off and Sediment in a Forested Watershed. *Hydrol. Process.* 29, 481–
630 497.

631 Salesa, D., Cerdà, A., 2020. Soil erosion on mountain trails as a consequence of recreational
632 activities. A comprehensive review of the scientific literature. *J. Environ. Manage.* 271.
633 <https://doi.org/10.1016/j.jenvman.2020.110990>

634 Senanayake, S., Pradhan, B., 2022. Predicting soil erosion susceptibility associated with
635 climate change scenarios in the Central Highlands of Sri Lanka. *J. Environ. Manage.*
636 308, 114589. <https://doi.org/10.1016/j.jenvman.2022.114589>

637 Smetanová, A., Follain, S., David, M., Ciampalini, R., Raclot, D., Crabit, A., Le Bissonnais,
638 Y., 2019. Landscaping compromises for land degradation neutrality: The case of soil
639 erosion in a Mediterranean agricultural landscape. *J. Environ. Manage.* 235, 282–292.
640 <https://doi.org/10.1016/j.jenvman.2019.01.063>

641 Tarafdar, P.K., Ray, R., 2005. Effect of trees on improvement of physical environment and
642 fertility in soils of West Bengal. *Bull. Nat. Inst. Ecol* 16, 129–136.

643 Torri, D., Poesen, J., Borselli, L., 1997. Predictability and uncertainty of the soil erodibility
644 factor using a global dataset. *Catena* 31, 1–22.

645 Veihe, A., 2002. The spatial variability of erodibility and its relation to soil types: a study
646 from northern Ghana. *Geoderma* 106, 101–120.

647 Wang, G., Gertner, G., Liu, X., Anderson, A., 2001. Uncertainty assessment of soil erodibility

648 factor for revised universal soil loss equation. *Catena* 46, 1–14.

649 Wang, X., Sun, L., Zhao, N., Li, W., Wei, X., Niu, B., 2022. Multifractal dimensions of soil
650 particle size distribution reveal the erodibility and fertility of alpine grassland soils in the
651 Northern Tibet Plateau. *J. Environ. Manage.* 315, 115145.
652 <https://doi.org/10.1016/j.jenvman.2022.115145>

653 Williams, J.R., Renard, K.G., Dyke, P.T., 1983. EPIC: A new method for assessing erosion's
654 effect on soil productivity. *J. Soil water Conserv.* 38, 381–383.

655 Wischmeier, W.H., Smith, D.D., 1978. Predicting rainfall erosion losses: a guide to
656 conservation planning. Department of Agriculture, Science and Education
657 Administration.

658 Yang, X., Gray, J., Chapman, G., Zhu, Q., Tulau, M., McInnes-Clarke, S., 2018. Digital
659 mapping of soil erodibility for water erosion in New South Wales, Australia. *Soil*
660 *Research* 56, 158–170. <https://doi.org/10.1071/SR17058>

661 Young, R.A., Mutchler, C.K., 1977. Erodibility of some Minnesota soils. *J. Soil Water*
662 *Conserv.*

663

664